Early infection with white spot syndrome virus promotes changes in the gut microbiome and immune-energy related genes of shrimps *Litopenaeus vannamei* (Boone, 1931)

doi: 10.22201/fmvz.24486760e.2025.1377

Section: Original Resarch

Frank Miguel Segura-Cadiz[1]
0000-0002-6487-0000

Jesús Alejandro Zamora-Briseño[2]
0000-0003-2079-9676

Ariadne Hernández-Pérez[3]
0000-0002-4908-4466

Jorge Luis Montero-Muñoz[1]
0000-0003-2463-1993

Juan Antonio Pérez-Vega[1]
0000-0002-4972-5040

Daniel Cerqueda-García[2]
0000-0003-1544-5662

Manuel Ángel Valenzuela-Jiménez[4]
0000-0002-1738-2282

Gabriela Gaxiola Cortés[4]
0000-0001-6260-9653

Rossanna Rodríguez-Canul[1]*
0000-0003-0469-1489

[1] Instituto Politécnico Nacional. Centro de Investigación y de Estudios Avanzados-Unidad Mérida. Departamento de Recursos del Mar. Mérida, Yucatán, México.

[2] Instituto de Ecología, A. C. Red de Estudios Moleculares Avanzados, Campus III. Xalapa, Veracruz, México.

[3] Universidad Nacional Autónoma de México. Facultad de Medicina Veterinaria y Zootecnia. Departamento de Medicina y Zootecnia de Abejas, Conejos y Organismos Acuáticos. Ciudad de México, México.

[4] Universidad Nacional Autónoma de México. Facultad de Ciencias. Unidad Multidisciplinaria de Docencia e Investigación-Sisal. Puerto de Sisal, Yucatán, México.

*Corresponding author: rossana.rodriguez@cinvestav.mx

Dates:

Submitted: 2024-07-21
Accepted: 2025-03-11
Published: 2025-05-13

Cite this as:

Segura-Cadiz FM, Zamora-Briseño JA, Hernández-Pérez A, Montero-Muñoz JL, Pérez-Vega JA, Cerqueda-García D, Valenzuela-Jiménez MA, Gaxiola Cortés G, Rodríguez-Canul R. Early infection with white spot syndrome virus promotes changes in the gut microbiome and immune-energy related genes of shrimps *Litopenaeus vannamei* (Boone, 1931). Veterinaria Mexico OA. 2025;12.

doi: 10.22201/fmvz.24486760e.2025.1377.

Early infection with white spot syndrome virus promotes changes in the gut microbiome and immune-energy related genes of shrimps *Litopenaeus vannamei* (Boone, 1931)

Abstract

The white spot syndrome virus (WSSV) is currently the main threat to the shrimp industry due to significant economic losses associated with shrimp mortality. The first hours of host-parasite interactions are crucial for the fate of WSSV infection, which becomes irreversible after 72 h. During this critical period, there is still a limited understanding of the interaction between the gut microbiota and the host response. In this study, we evaluated the effect of WSSV on the Pacific white shrimp *Litopenaeus vannamaei* (Boone, 1931) at the gut microbiome level and the expression of four genes in hemocytes and hepatopancreas associated with aerobic (ATP synthase) and anaerobic (LDH) metabolism, cell pathogen internalization (AP-2), and immune response (α2M). The genes LDH and α2M were overexpressed in hemocytes and hepatopancreas, while the AP-2 gene was overexpressed only in hemocytes. In infected shrimps, we observed a positive correlation between the increase in viral load (VL), the upregulation of the genes LDH and AP-2, and the augmentation of the relative abundance of *Ideonella*, *Actinobacter*, *Flavobacterium*, *Caldalkalibacillus*, *Gemmobacter*, *Pirellula*, *Metilophylus,* *Hydrogenophaga*, *Pseudomona*, *Methylophaga*, *Candidatus Bacilloplasma,* and *Novosphingobium*. Whereas the gut microbiome in uninfected shrimps was represented by *Motilimonas*, *Tamlana*, *Shimia*, *Spongiimonas*, *Pseudoalteromonas*, *Aeromones,* and

Shewanella. Results from this study contribute to understanding the intricate interplay between WSSV infection, the host response, and gut microbiota in aquaculture settings.

Keywords: *Litopenaeus vannamei*; Immune system; WSSV-*Ie* gene; Early genes; Microbiome.

Study contribution

WSSV infection is the main cause of death in shrimps, or which there is no cure or treatment; and there is evidence that the first 48 h are crucial for the fate of the virus within its host. Intestinal microorganisms play an important role in maintaining host health, but their functions, along with changes in the gene expression profile during early WSSV infections, are unknown. We performed a comparative evaluation between experimentally infected and uninfected shrimps with WSSV in terms of viral load quantification, changes in the gut microbiota, and their correlations with the expression profile of genes associated with the anaerobic energetic metabolism, immune response, and cell-pathogen internalization. This study provided the first evidence that changes in gut microbiome are closely associated with the severity of WSSV infection and the expression profile of key genes that may help to monitor viral pathogenesis during the early stages of WSSV infection.

Introduction

Shrimp farming is one of the most economically relevant food industries worldwide, but it frequently suffers significant economic losses due to outbreaks associated with the white spot syndrome virus (WSSV), which has affected the global shrimp industry since its discovery in the early 1990s.[1] According to estimates, the cumulative economic impact of this virus is valued at 8 to 15 billion USD, and it is expected to increase.[2] WSSV is difficult to eradicate, in part because it has been reported in more than 100 host species from fresh, brackish, and marine waters.[3] Additionally, WSSV infection becomes irreversible at 72 hours post-infection, causing mortality within 3 to 10 days. Thus, evaluating the prognosis of the infection during early stages is crucial, either for diagnosis or for linking the host response, through gene expression analyses, with changes in the gut microbiome, in search of additional strategies to control WSSV.

Infection begins when virions bind to the surface of a target cell.[4] During this interaction, the first few hours of infection are crucial for both the virus and its host. After penetrating the cell membrane of target cells, WSSV particles are located within early endosomes.[5] Clathrin-mediated endocytosis occurs at specialized sites where viruses bind to specific receptors.[6] The coated pits then invaginate and form intracellular clathrin-coated vesicles. Clathrin assembly requires the heterotetrameric protein complex AP-2, which contains four subunits: α, β2, μ2, and σ2.[7–9]

Then, WSSV particles escape from the endosome to the cytosol through membrane fusion or membrane disruption mechanisms.[9] They then reach the nucleus and penetrate the nuclear envelope within the first twelve hours post-infection (hpi).[10] Inside the nucleus, the virus begins to express its own genes to initiate its replication using

the host's replication machinery. In these circumstances, "early genes", which encode transcription factors and other regulators that enable the transcription of viral genes, are activated. Subsequently, "late genes" are expressed after the initiation of viral DNA synthesis and the formation of structural proteins.[10, 11]

Additionally, during WSSV infection, the expression of a wide range of genes in the host is altered, especially those related to the immune response and cellular processes.[12, 13] The cellular processes associated with immune defense include energy production, clathrin-mediated transport, protein transport, and protein synthesis.[13–15] For instance, it has been reported that the virus manipulates the host's energy metabolism to initiate viral colonization and replication.[13] Two examples of enzymes involved in energy metabolism are L-lactate dehydrogenase (LDH) and ATP synthase. LDH produces lactate from pyruvate in the last step of glycolysis, regulating the rapid production of large amounts of energy.[16, 17] In invertebrates, LDH expression is regulated under hypoxia, viral infections, and exposure to several xenobiotics.[16, 18] Another example is the ATP synthase, which plays a central role in ATP synthesis. ATP synthase has been found on the surface of hemocytes in the crayfish *Pacifastacus leniusculus* and *L. vannamei*.[19, 20] The enzyme alpha-2-macroglobulin (α2M) is one of the most abundant and multifunctional proteins in shrimp and is a broad-spectrum inhibitor of serine proteinase.[21] This enzyme is involved in several immune responses in invertebrates, such as phagocytosis, hemolymph coagulation, and prophenoloxidase activation.[22, 23]

The gut microbiota is crucial for the immune development and maintenance of host metabolism.[24, 25] The gut microbiome is a complex microbial community comprising approximately 100 trillion microorganisms in the digestive tract, influencing both host

metabolism and overall health.[26] Gut microbes have the potential to serve as biomarker for identifying specific signature during pathogenic invasion.[27] For example, during infections with fungi, white stool syndrome, and Acute Hepatopancreatic Necrosis Syndrome, significant changes occur in the composition and structure of the gut microbiota of infected shrimps compared to healthy individuals.[28–30] Additionally, in *L. vannamei*, WSSV infection leads to marked dysbiosis at 72 hpi, when the disease becomes irreversible.[31] However, evaluating disease progression during the early stages of WSSV infection –focusing on changes in the gut microbiome and the host response through alterations in the gene expression profile– would provide critical insights into the interaction between these factors and their impact on shrimp health. The primary aim of this study was to conduct a comparative evaluation between experimentally infected and uninfected shrimps with WSSV, analyzing viral load quantification and gut microbiota alterations during the early stages of infection (6, 12, 24, and 48 h) and their correlations with the expression profile of genes associated with energy metabolism (ATP synthase), anaerobic energy metabolism (LDH), innate immune response (α2M), and cell pathogen internalization (AP-2).

Materials and methods

Ethical statement

All live animal protocols described below were approved by the Comité Institucional de Cuidado y Uso de Animales of Centro de Investigación y de Estudios Avanzados (Cinvestav) (CICUAL-Cinvestav) under reference number: 0419-051. The procedures followed the guidelines established in the Mexican Official Standard NOM-062-ZOO-1999.

Viral inoculum preparation

The viral inoculum was prepared from gills, muscles, and pleopods of a WSSV-infected shrimp.[15, 32] Briefly, shrimp tissues were macerated and homogenized in 10 mL of sterile saline solution (150 mM NaCl), and centrifuged at 7 500 g/30 min/4 °C. The supernatant was then centrifuged again at 12 000 g/30 min/4 °C. After centrifugation, the supernatant was filtered through a 0.22 µm ultrafiltration membrane (Corning®), and the flow-through was concentrated using Amicon Ultra-15 Centrifugal Filter Units (Merck-Millipore®) with 100 kDa cut-off at 1 000 g/30 min/4 °C. The resulting material was used as the inoculum and stored at -80 °C until further use. The viral load was quantified by qPCR. The infectivity of the inoculum was verified in five healthy juvenile shrimps, which were injected intramuscularly with 100 µL of inoculum. Shrimps were monitored daily for the appearance of clinical signs of WSSV infection, such as erratic swimming, reduced food consumption, and reddish body coloration. After sacrifice, qPCR was performed to assess the viral load.

Exposure bioassay

For the exposure experiment, 80 juveniles *L. vannamei* were obtained from the aquaculture facilities of the Universidad Nacional Autónoma de México, Unidad Multidisciplinaria de Docencia e Investigación (UNAM-UMDI), Sisal. The organisms were transported to Cinvestav-Unidad Mérida and maintained for three weeks in filtered, aerated seawater [35 Practical Salinity Units (PSU)] in recirculated containers. Shrimp were fed twice daily with a commercial diet containing 35 % protein, at a feeding rate of 7 % of their biomass. The aquarium was cleaned daily to remove fecal matter and debris.

The organisms were acclimated for five days in 150 L tanks containing 35 PSU water at 26 ± 2 °C, pH 7.8 ± 0.3, with constant aeration. Then, 24 healthy juvenile shrimps (*L. vannamei*) (14.5 ± 2.5 g weight and 13.4 ± 0.6 cm lenght) were divided into control and experimental groups based on infection (6 hpi, 12 hpi, 24 hpi, and 48 hpi). Only intermolt-stage animals were used for the experiments. The organisms were assigned to a control group (n = 36) and an experimental group (n = 36). Shrimps in the experimental group were injected intramuscularly between the third and fourth abdominal segments using a 1 mL insulin syringe, containing 100 µL (~2.16×10^6 viral copies) of the WSSV inoculum. The organisms in the control group were injected with a sterile saline solution. Three individuals from the control group and three from the experimental group were collected at 6 hpi, 12 hpi, 24 hpi and 48 hpi for subsequent analyses.

Sample collection

Hemolymph was extracted from the ventral hemolymphatic sinus using an insulin syringe preloaded with 750 µL of anticoagulant shrimp solution (SC-EDTA pH 7.2, 900 mOsm/L) at a 3:1 ratio (anticoagulant-hemolymph).[33] The hemolymph-anticoagulant mixture was centrifuged at 1 000 g/ 7 min. The supernatant was discarded, and the pellet was resuspended with 500 µL of SC solution. It was then centrifuged again, and the resulting pellet (hemocytes) was immediately fixed with TRizol reagent (Thermo Scientific©) and stored at -80 °C until analysis.

The shrimps body surface was washed with sterile water and 75 % ethanol before dissection. Gills and intestines were fixed in 96° ethanol for genomic DNA (gDNA)

extraction. A ~2 g piece of hepatopancreas and hemocytes were preserved in RNA later (Invitrogen). All samples were immediately stored at −80 °C until further use.

Genomic DNA extraction

gDNA was extracted from gill and intestine samples using the Quick-DNA™ Miniprep Plus (Zymo Research™) kit. DNA concentration and purity were assessed spectrophotometrically. The quality and integrity of the total DNA were evaluated by gel electrophoresis (1 % agarose gel), and the DNA was stored at −20 °C until analysis.

Viral load quantification

The viral load of the inoculum and samples was determined by qPCR using a standard curve. The qPCR assays were performed using a Rotor-Gene Q (QIAGEN®) thermocycler and the QuantiNova SYBR Green PCR Master Mix (QIAGEN®). Each reaction consisted of 7.5 µL 2× QuantiNova SYBR Green (QIAGEN®), 2 µL of each dilution or 50 ng of gDNA template, 0.5 µL of each primer (5 µM) and 4.5 µL of nuclease-free water. The reaction conditions were initial denaturation step of 95 °C/ 3 min, 30 cycles of 95 °C/ 30 s, 59 °C/ 30 s and 72 °C/ 30 s, with a final extension at 72 °C for 5 min. Amplification specificity was assessed by melting curve analysis. Additionally, a calibration curve was prepared with 1:10 dilutions of plasmid DNA for quantification.

The primers used in the qPCR were *Ie*-126Fw (TGAAACGGTGTGCTGTTAGC) and *Ie*-126Rv (AAGTTCCTCCATCGTCATCG) for the early infection gene [GenBank Accession number (AN) = GE616383.1] and VP28-140Fw (CTGCTGTGATTGCTGTATTT) and VP28-140Rv (CAGTGCCAGAGTAGGTGAC)

(AN = AY422228.1), targeting the capsid protein gene, which is the reference gene recommended by World Organisation of Animal Health (WOAH) and used here as the positive control.[15]

Plasmid DNA was obtained from recombinants bacteria (*Escherichia coli*) preserved in glycerol and cloned with either the *Ie*1-126 gene or the Vp28-140 gene. These bacteria were reconstituted and cultured on LB solid medium supplemented with ampicillin (selective medium). Plates were incubated overnight at 37 °C. From this microbial growth, an isolated colony was selected and inoculated in LB liquid medium supplemented with 10 µL of ampicillin and incubated at 37 °C with shaking for 14-16 h to ensure optimal microbial growth. The cultured bacteria were centrifuged at 14 000 rpm for a minute to pellet the biomass. The plasmids were purified using the GeneJET Plasmid Miniprep Kit (Thermo Fisher Scientific™). The presence and integrity of plasmid DNA were verified by 1 % agarose gel electrophoresis (**Supplementary Figure 1**). The qPCR data were processed using software Rotor-Gene version 6.1.

RNA extraction and complementary DNA obtention

RNA was extracted from hemocytes and hepatopancreas using the Direct-zol RNA kit (Zymo Research©). RNA purity and integrity were assessed using a NanoDrop™ 2 000c (Thermo Scientific©) and 1 % agarose gel electrophoresis. Then, all RNA samples were standardized to a final concentration of 100 ng/µL for complementary DNA (cDNA) synthesis by reverse transcription-quantitative polymerase chain reaction (RT-qPCR), using the High-Capacity cDNA Reverse Transcription Kit (Thermo Fisher Scientific™).

Primer calibration curves were generated using five serial dilutions with a 1:5 dilution factor.

Gene expression analyses by qPCR

Four genes related to energy metabolism and immune response were quantified:

- L-lactate dehydrogenase isoform X2 (LDH), associated with anaerobic metabolism.[18]
- ATP synthase subunit mitochondrial (ATP), associated with aerobic metabolism and the energy production pathway.[20, 34−36]
- AP-2 complex subunit alpha (AP-2), associated with protein transport, clathrin-mediated endocytosis.[7−9, 37]
- Alpha-2-macroglobulin isoform X3 (α2M), involved in the immune response as a protease inhibitor.[21−23, 38]

The reference gene glyceraldehyde-3-phosphate dehydrogenase (GAPDH), was selected as an internal control "housekeeping" gene (**Table 1**).[39]

Table 1. Primers used for the gene expression analyses in uninfected and WSSV-infected *L. vannamei*

Gene	Primer name	Sequence Forward (5'- 3') Reverse (3'- 5')	Function	Access number (GenBank)
Glycoaldehyde-3-phosphate dehydrogenase	*GAPDH*	F:CCATGGAATGTTCTCGGGCT R:AAGTATGACAGCACACGG	Housekeeping	GETZ01023697.1
L-lactate dehydrogenase isoform X2	*LDH*	F: GACGAGCACCAGCTAACA R: AAGCTGCGTGGAGATGAT	Response to hypoxia and physiological stress, anaerobic metabolism, rapid energy production.	GETD01035385.1
ATP synthase subunit mitochondrial	*ATP*	F: GCAGGTGATGTCCCTTCAT R: GACAATGCCAGAGCTCAA	Aerobic metabolism and energy generation.	GCVY01000156.1
AP-2 complex subunit alpha	*AP-2*	F:TCATCTGTGCCGTCTGAGTC R:TCTTCCATCTTAGCGGTGCT	Protein transport, clathrin-mediated endocytosis.	GETD01037536.1
Alpha-2-macroglobulin isoform X3	*α2M*	F: ACACATCCAGATGGTGAA R: CAACCACATAAGCTGCAA	Protease inhibitor, regulator of the immune response of invertebrates.	GETZ01051103.1

Gene expression quantification was performed by qPCR using a Rotor-Gene Q thermocycler (QIAGEN®), and the Máxima SYBR Green/ROX qPCR Master Mix/2X kit (Thermo Fisher Scientific™). Reactions were standardized to a final volume of 10 µL containing:

- 5 µL of Maxima SYBR Green 2X (QIAGEN®).
- 0.625 µL of diluted cDNA (prepared as 5 µL of cDNA + 20 µL of nuclease-free water).
- 0.21 µL of each primer (5 µM)
- 3.96 µL of nuclease-free water.

The thermal cycling conditions for amplification included an initial denaturation at 95 °C for 10 min, followed by 35 cycles of:

- Denaturation at 95 °C for 10 s.
- Extension at 60 °C for 45 s.

All data were processed using Rotor-Gene Q software version 2.1.0.9 (Windows platforms). To confirm the specificity of the amplification, a dissociation curve analysis of the generated products was performed.

Amplification and sequencing of 16S rRNA gene

The V3-V4 hypervariable regions of the bacterial 16S rRNA gene were amplified from intestine samples by PCR, using the primer pair:

- 16S rRNA Forward Primer:

  5'TCGTCGGCAGCGTCAGATGTGTATAAGAGACAGCCTACGGGNGGCWGCAG

- 16S rRNA Reverse Primer:

  5'GTCTCGTGGGCTCGGAGATGTGTATAAGAGACAGGACTACHVGGGTATC

  TAATCC

These primers generated ~550 bp amplicons.[40] DNA from nine organisms was pooled into groups of three and analyzed.

The PCRs reactions were performed using a C1000 Touch™ Thermal Cycler (Bio-Rad Laboratories Inc., USA) in a 25 µL total reaction volume containing:

- 12.5 µL of 2× DreamTaq Green PCR Master Mix (Thermo Scientific),
- 2.5 µL of gDNA template,
- 0.1875 µL (125 nM) of each primer,
- 9.6 µL of nuclease-free water.

The thermal cycling conditions were as follows:

- Initial denaturation at 95 °C for 3 min.
- 30 cycles of:
  - Denaturation at 95 °C for 15 s,
  - Annealing at 53 °C for 30 s,
  - Extension at 72 °C for 60 s,
- Final extension at 72 °C for 7 min.

Amplification specificity was confirmed by melting curve analysis. Additionally, a calibration curve was generated using 1:10 serial dilutions of plasmid DNA for quantification. The quality and integrity of the PCR products were evaluated using 1 % agarose gel electrophoresis. PCR products were stored at -20 °C.

Libraries were prepared following the 16S Metagenomic Sequencing Library Preparation protocol from Illumina©. The concentration of libraries was assessed by Qubit 2.0 Fluorometer (Thermo©, USA). Amplicons were purified using AMPure XP beads and indexed with Illumina sequencing adapters using the Nextera XT Index Kit. Indexed amplicons were further purified and quantified as previously described. The library quality was assessed using an Agilent Bioanalyzer 2100 system. Indexed amplicons were sequenced in a paired-end (2 × 300 bp) with a MiSeq Reagent Kit V3 (600 cycles), on the MiSeq platform (Illumina, San Diego, CA, USA). Sequencing was conducted at the Sequencing Unit and Polymorphims Detection, Inmegen, Mexico.

Data analysis

The quantification of gene expression was carried out in a relative manner.[41, 42] The gene expression profile (mRNA relative quantification), was analyzed using comparative quantification analysis according to the Pfaffl method, implemented in REST-2009 software v. 2.0.13. Relative expression values were obtained by comparing experimental groups with the control group, for both reference and target genes. The mathematical model used is based on real-time PCR efficiencies and the mean crossing point deviation between samples and the control group. The expression ratio results of the investigated transcripts were tested for significance using a randomization test (2000 permutations), with a type I error used was $\alpha = 0.05$.[43] Samples were analyzed in triplicate and plotted using GraphPad Prism® v.8.0.1 (GraphPad Software, San Diego, California USA, www.graphpad.com).[43, 44]

For the metagenomic analysis, paired-end reads (2 × 300 bp) were processed with the QIIME2 pipeline (https://qiime2.org).[45] The demultiplexed FASTQ files were processed with the DADA2 plugin.[46] Sequences were trimmed at position 20 in the 5' end and truncated at position 280 in the 3' end for both forward and reverse reads. Reads were denoised, amplicon sequences variants (ASVs) were resolved, and chimeric sequences were removed using the "consensus" method. The taxonomy of representative ASV sequences was assigned using the QIIME plugin feature-classifier classify-consensus-vsearch (v2.9.0).[47] The SILVA database (version 132) was used for classification. ASV representative sequences were aligned using the MAFFT algorithm. After positional conservation and gap filtering, phylogenetic tree was built using the FastTree algorithm. Mitochondrial and chloroplast ASVs were removed, and the feature table was rarefied to a sequencing depth of 9 999.

The featured table and tree were exported R (http://www.R-project.org/) and statistical analyses were performed using the phyloseq, ggplot2 and vegan package. A PERMANOVA test was conducted to determinate the β diversity. Additionally, a linear discriminant analysis (LDA) effect size (LEfSe)[48] was performed at the ASV level to identify microbial taxa with differential abundances among treatments, using a LDA cut-off > 2 and a Kruskal-Wallis alpha value 0.05.

Using the database from the experimental and control groups at different time points, a non-Euclidean triangular dissimilarity matrix was calculated based on differential percentages of bacterial abundance (Bray Curtis coefficient).[49] This matrix was used in the principal coordinate analysis (PCoA). In this ordination analysis, a Euclidean representation of objects (rows) was generated, where relationships were measured using

a dissimilarity metric. The PCoA analysis was performed using the cmdscale fuction with Cailliez correction from the vegan package [50], version 6-4, in R (R Development Core Team, 2023). Finally, to evaluate the correlations of independent variables (LV, AP-2 and LDH) with change in the composition and structure of bacterial genera from control and experimental groups, we used the envfit function from the vegan library in R.[50] The envfit function gives computes the squared correlation coefficient, using 9 999 random permutations for statical testing.

Results

Viral load quantification

In the inoculum, ~40 000 viral copies/µL were detected (**Supplementary Figure 2**). Following Koch´s postulates, after 24~48 hpi, five shrimps infected with the inoculum started to exhibit typical signs of the disease, such as:

- Reduced feed consumption
- Lethargy and erratic swimming
- Cuticle loss
- Reddish body coloration[3]

Genomic DNA extraction and viral quantification in gills

The gDNA concentration ranged between 100~250 ng/µL, and gDNA purity was between 1.85–2, in all samples at different infection time points. The viral load of WSSV increased over time. Amplification specificity was confirmed by melting curve analysis (**Supplementary Figure 1**).

Using the *Ie*1-126 primers:

- ~10 viral copies were detected at 6 hpi
- ~300 viral copies were detected at 12 hpi
- ~700 viral copies were detected at 24 hpi
- ~330 000 viral copies/µL were detected at 48 hpi (**Figure 1a**).

Using the Vp28-140 primers:

- No viral copies were detected at 6 hpi
- ~10 viral copies were detected at 12 hpi
- ~25 viral copies were detected at 24 hpi
- ~38 000 viral copies were detected at 48 hpi (**Figure 1b**)

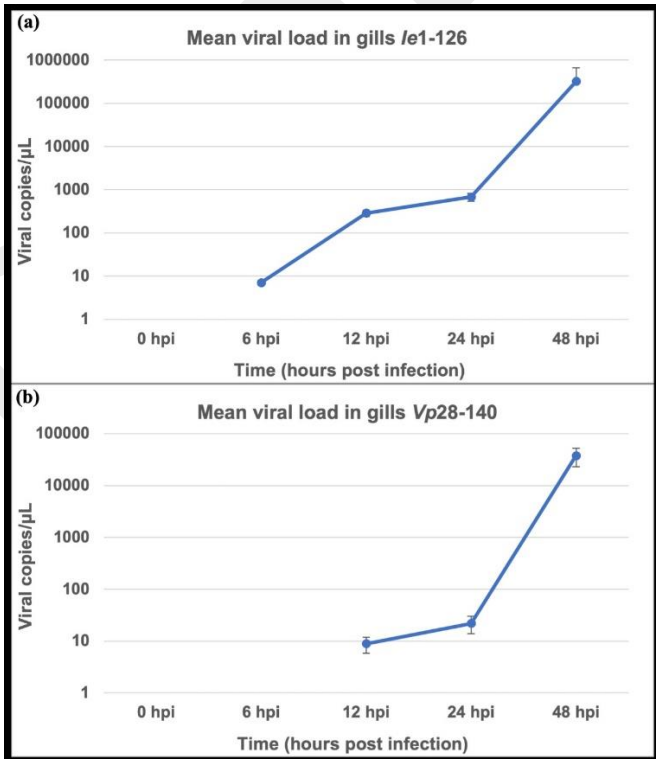

Figure 1. Time-course infection of WSSV in *L. vannamei*. At 6, 12, 24, and 48 hpi, concerning the negative control for (a) the early infected gene: *Ie*1-126 and (b) the Vp28-140 genes. hpi: hours post-infection.

Gene expression analyses

The gene expression profile of LDH, AP-2, α2M, and ATP synthase exhibited distinct patterns throughout the infection time course. The LDH, AP-2, and α2M genes were upregulated, whereas the ATP synthase gene did not show any significant changes in any of the samples. Specifically, the LDH gene exhibited a high level of upregulation in hemocyte samples compared to hepatopancreatic samples from 12 to 48 hpi, with significant differences ($P = 0.01812$) compared to the control. The ATP synthase gene showed no significant changes in any of the tested samples. The AP-2 gene was upregulated in hemocytes at 48 hpi ($P = 0.0023$), while no upregulation was observed in the hepatopancreas. Finally, the α2M gene was upregulated in hemocytes at 24 hpi ($P = 0.0236$), and 48 hpi ($P \leq 0.05$), while in the hepatopancreas it was upregulated only at 48 hpi with lower values but significantly different from the control ($P = 0.0321$) [**Figure 2**].

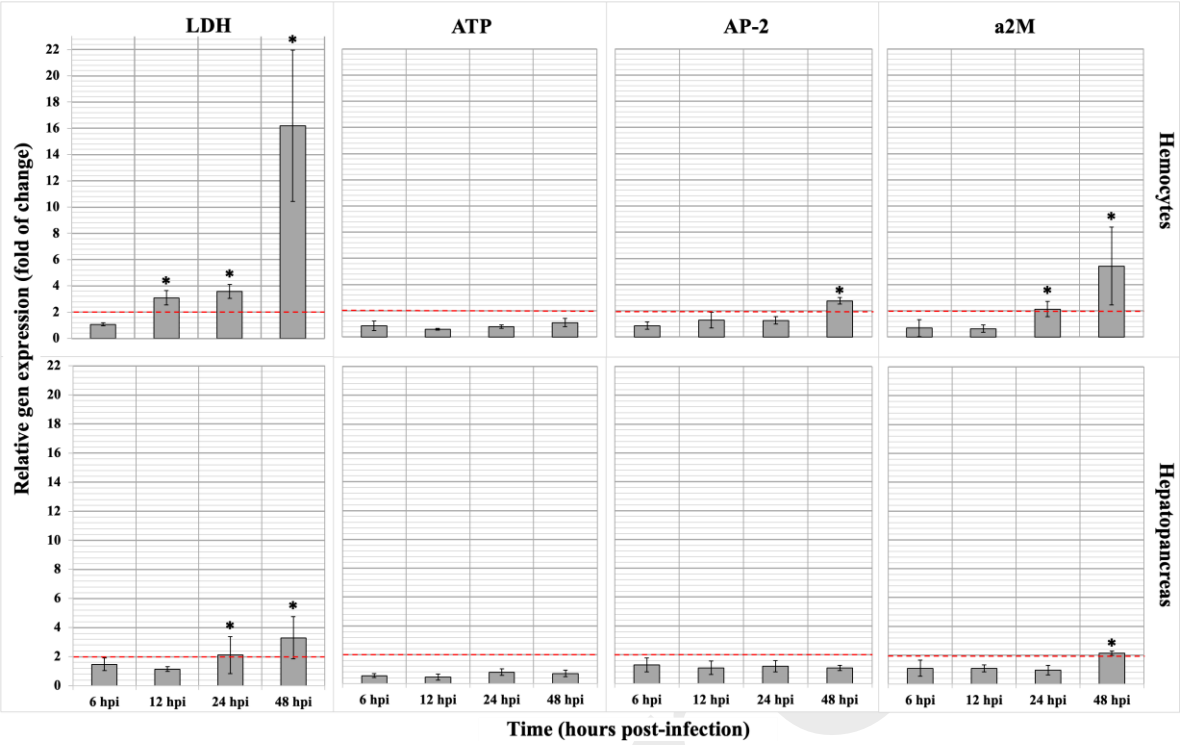

Figure 2. Relative gene expression values for LDH, ATP synthase, AP-2, and α2M genes in hemocytes and hepatopancreas, error bars represent standard deviations, identified with an asterisk (*) the samples with significant differences for the control and the lower dotted line marks the limit from which the fold change is considered significant and by which it can be determined whether the gene is or not overregulated or deregulated. The type I error used was α=0.05. LDH: L-lactate dehydrogenase isoform X2, ATP: ATP synthase subunit mitochondrial, AP-2: AP-2 complex subunit alpha, α2M: Alpha-2-macroglobulin isoform X3). hpi: hours post-infection.

Amplification and sequencing of 16S rRNA gene

Genomic DNA was extracted from intestinal samples, and the V3-V4 hypervariable regions of the bacterial 16S rRNA gene were amplified. All PCR products had a concentration range between 100–200 ng/µL and a purity range between 1.9–1.99. The

sequencing analysis of 16S rRNA amplicons yielded a total of 1 825 641 sequence reads from WSSV-infected shrimps gut samples. However, after filtering, only 743 992 high-quality reads were retained for taxonomic classification.

Analysis of the composition and structure of bacterial communities

The sequencing analysis identified 30 bacterial genera (521 ASVs) in the gut samples (**Figure 3**). The most abundant genera were *Vibrio*, *Shewanella*, *Pseudomonas*, *Aeromonas,* and *Flavobacterium* (**Figure 3**).

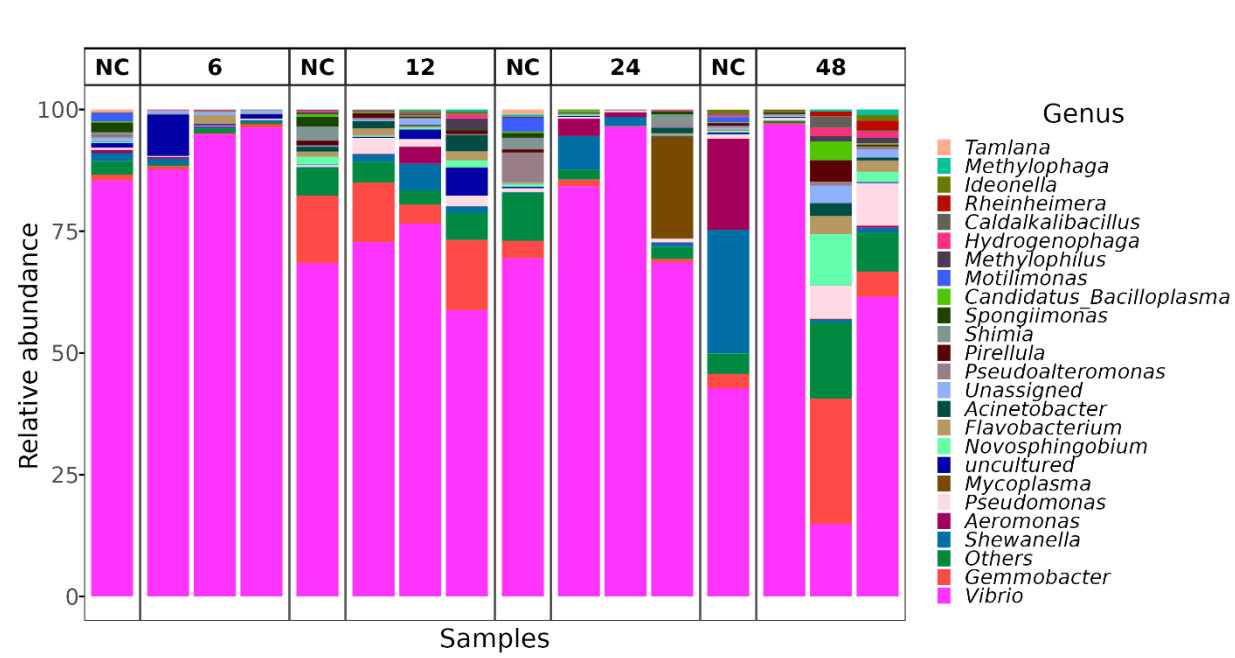

Figure 3. Abundance of genera diversity obtained by 16S rRNA amplicons sequencing analysis of the intestine samples of White Spot Syndrome Virus (WSSV)-infected shrimps. Shrimps were analyzed at 6, 12, 24, and 48 hpi (hours post-infection), to their negative control (NC).

The intestines of infected shrimps were represented by individual variability associated with *Vibrio parahaemolyticus*, but at 48 hpi *Pseudomonas stutzeri* was observed. In the β diversity analysis, no significant differences were observed between the negative control (F = 1.1618, R2 = 0.297, P = 0.201) (**Figure 4**).

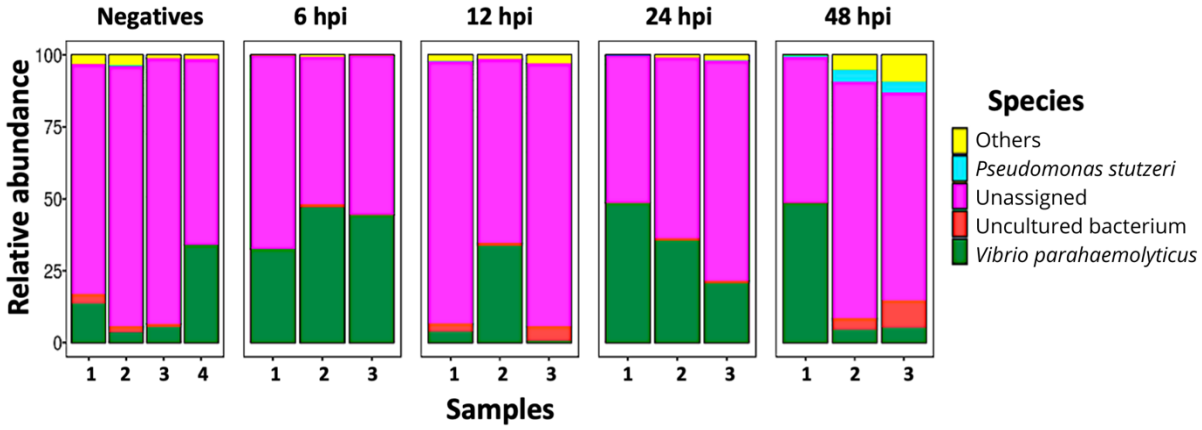

Figure 4. Relative abundance of species diversity obtained by 16S rRNA amplicons sequencing analysis of intestine samples of WSSV-infected shrimps. hpi: hours post infection.

Differential abundance analysis between healthy and WSSV-infected shrimps

Significative differences in the relative abundance by genera were observed between WSSV-infected shrimps and controls by LefSe analysis (**Figure 5**). A great abundance of *Vogesella* and *Cloacibacterium* were observed in WSSV-infected shrimps to non-infected, while *Vibrio*, *Pseudomonas*, *Shimia*, *Pseudoalteromonas*, *Tenacibaculum*, *Colwellia,* and *Celeribacter* genera were more abundant in the non-infected shrimps than in the WSSV-infected shrimps.

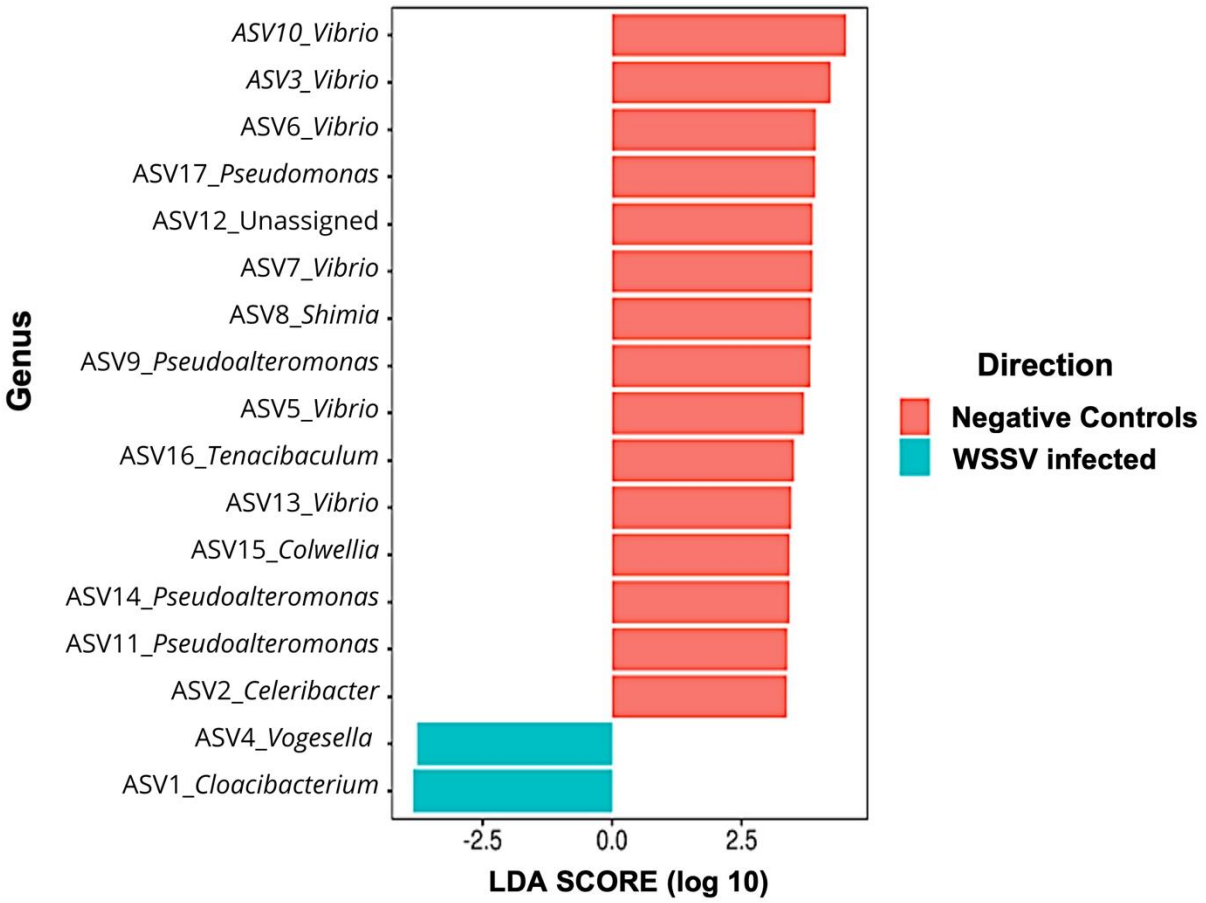

Figure 5. Linear discriminant analysis (LDA) effect size (LEfSe) showed significant differences in genera abundance observed between WSSV-infected shrimps and non-infected shrimps from negative controls.

In principal coordinate analysis (PCoA) was applied the non-Euclidean triangular dissimilarity matrix, calculated using the percentage difference (Bray-Curtis) coefficient. The genus of each microorganism and the analyzed variables are shown in **Supplementary Table 1**. **Figure 6** illustrates changes in the composition and structure of the bacterial genera over different experimental time points. The greatest change (dissimilarity) occurs at 48 h, due to an increase in the abundance and diversity of

bacteria. Therefore, the increase in dissimilarity at 48 h is positively correlated with the expression of the genes:

- LDH (r2 = 0.6031, P = 0.0180)
- AP-2 (r2 = 0.6332, P = 0.0156)
- Viral load [VL (r2 = 0.5189, P = 0.0398)]

At this time point, microbiome analyses, showed that the relative abundance in the control group was dominated by: *Motilimonas* (MTM), *Tamlana* (TAM), *Shimia* (SHI)*, Spongiimonas* (SPG), *Pseudoalteromonas* (PAM), *Aeromones* (ARM), and *Shewanella* (SHW). In contrast, in WSSV infected shrimps, we observed a positive correlation between the rise in viral load (VL), and the upregulation of the LDH and AP-2 genes, along with and increased relative abundance of: *Ideonella* (IDN), *Actinobacter* (ATB), *Flavobacterium* (FVB)*, Caldalkalibacillus* (CKB), *Gemmobacter* (GMB), *Pirellula* (PIR), *Metilophylus* (MTP), *Hydrogenophaga* (HGP), *Pseudomona* (PDM), *Methylophaga* (MTP), *Candidatus Bacilloplasma* (CBP), and *Novosphingobium* (NPG). The relative abundance of *Mycoplasma* (MYC) *a*nd *Vibrio* (VIB) was specifically associated with an increase in viral infection.

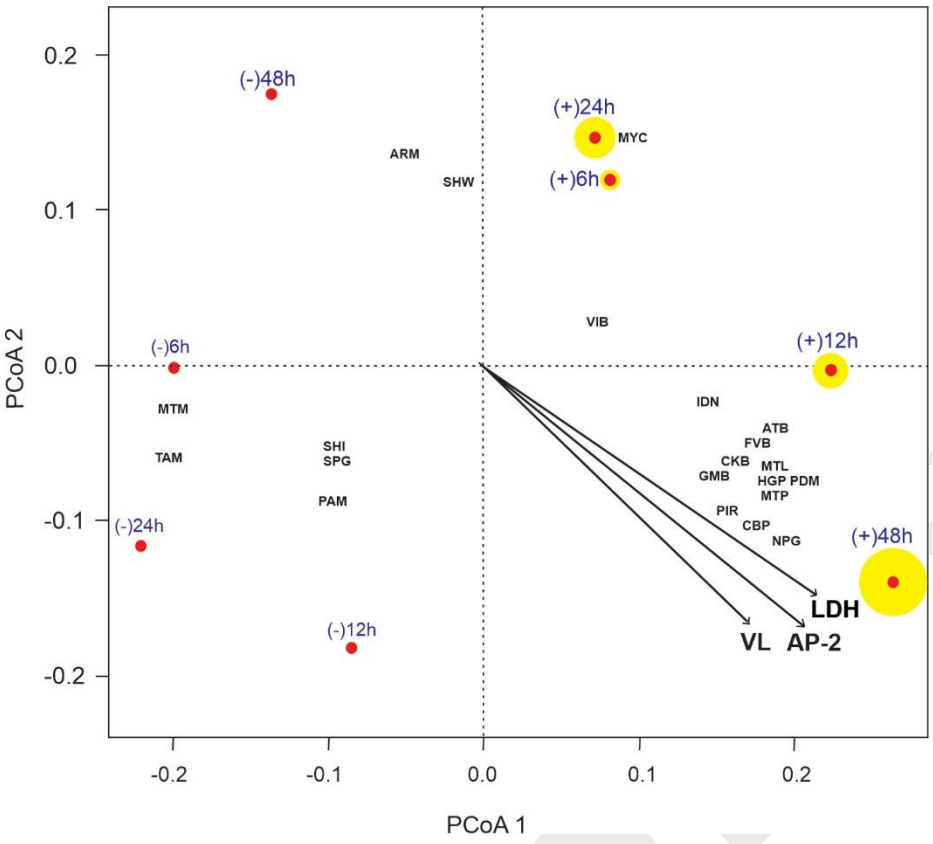

Figure 6. Principal coordinate analysis (PCoA). Ordination analysis shows that at 48 hours post-inoculation (hpi) a greater composition of bacteria is observed when compared to the other experimental times and controls. The vectors show a positive correlation of the expression of the genes L-lactate deshydrogenase isoform X2 (LDH) (r2 = 0.6031, P = 0.0180), AP-2 complex subunit alpha (AP-2) (r2 = 0.6332, P = 0.0156) and viral load [VL (r2 = 0.5189, P = 0.0398)], with the change in composition of bacterial genera (greater dissimilarity) at 48 hpi. The size of the yellow circle is proportional to the viral load.

Discussion

In the WSSV-shrimp interaction, the first 48 h are essential for the virus to accomplish the transcription of its genetic material. During this process, the virus employ strategies to evade the immune system and enter the cell for subsequent replication.[51–53] The viral load detection of WSSV using the *Ie*1-126 primers increased from ~10 viral copies/µL at 6 hpi to ~330 000 viral copies/µL at 48 hpi, while the Vp28-140 primers detected from ~10 viral copies/µL at 12 hpi, to ~330 000 viral copies/µL at 48 hpi. *Ie*1 genes function as active trans-regulation factors to initiate viral replication during WSSV infection.[15, 54, 55] In contrast, the envelope protein Vp28 plays a key role in the infection process.[56] Vp28 primers are currently used as reference genes by the World Organisation for Animal Health to confirm an active infection.[57] However, the implementation of diagnostic tests using *Ie*1 primers would also be useful for detecting early WSSV infections in aquaculture settings.[51]

In the gene expression analyses, the ATP synthase gene showed no significant changes. Our results align with similar studies where ATP synthesis activity after WSSV infection was inhibited.[20, 36] ATP is rapidly consumed due to the rapid replication of WSSV in host cells, interfering with other energy-dependent biological functions of the host.[34, 58] When the aerobic pathway is suppressed, the anaerobic alternative pathway for energy production is activated. In this study, a marked upregulation of LDH gene and α2M genes was observed in hemocytes compared to the hepatopancreas. Our results are consistent with other studies on hemocytes of WSSV-infected shrimp.[18, 59] During the infection process, WSSV interferes with glycolysis (the glucose degradation pathway).[59, 60] The mechanism by which WSSV infection impairs glycolysis may involve

the alteration of LDH activity.[17, 18] LDH plays a crucial role in the rapid production of large amounts of energy and is upregulated mainly under hypoxic conditions or when there is an immediate energy demand.[17, 61]

Also, in invertebrates, α2M (α-2-macroglobulin) is associated with immune defense mechanisms.[62, 63] The overexpression of α2M in hemocytes and hepatopancreas observed here may be related to the increase in endogenous proteases in response to pathogens invasion.[63–67] It has also been described that α2M may facilitate the entry of phagocytosis-activating proteins into phagocytic cells, enhancing immunity in infected shrimps[68] or during stress associated with the effect of abiotic conditions.[69]

On the other hand, AP-2 gene was only upregulated in hemocytes. WSSV uses a well-characterized cellular endocytic mechanism to internalize in cells through a clathrin-mediated endocytosis, which has been proposed as the principal strategy of internalization in shrimp cells.[14] Clathrin assembly to form coated pits requires the heterotetrameric protein AP-2.[7, 8] Here, the upregulation of AP-2 in hemocytes benefits entry into the cell via clathrin-dependent endocytosis. It has been reported that inhibition of the clathrin pathway could delay WSSV proliferation, as clathrin-mediated endocytosis is essential for WSSV infection.[14, 70] This is a topic that deserves further evaluations, as our findings suggest that studying this signaling pathway in WSSV-susceptible and WSSV-resistant hosts could help develop strategies to block viral entry pathways.

In uninfected shrimps, the intestinal microbiota is mainly composed of the genera *Vibrio*, *Aeromonas,* and *Shewanella*,[71–74] which is consistent with our findings. The genus *Vibrio* is common in the digestive track of shrimp,[71, 72, 74–76] and its predominance in healthy shrimp suggests that these bacteria may act as opportunistic agents capable of

causing disease when gut microbiota balance is disrupted.[31, 77] For this reason, the abundance of *Vibrio* species is routinely monitored to qualitatively estimate disease risk in shrimp farms.[78–80] The genus *Aeromonas* was also abundant and is considered an opportunistic pathogen in shrimp and fish.[78, 81, 82] Its presence in the intestines of infected shrimp has been associated to dysbiosis.[83 84] In contrast, the genus *Shewanella* is used as a probiotics to promote nutrition, diseases resistance, and other beneficial activities.[85, 86]

In infected shrimps, the relative abundance of the genera *Vogesella* and *Cloacibacterium* increased. To date, there are no reports of the role of these microorganisms in shrimp intestine, although these species have been reported in sewage and wastewater.[87] On the other hand, the genera *Vibrio*, *Pseudomonas*, *Pseudoalteromonas*, *Shimia*, *Tenacibaculum,* and *Colwellia* significantly decreased in infected organisms. This reduction may reflect a decrease in intestinal metabolism, affecting the overall health of the organism.[88, 90] *P. stutzeri* has been reported in denitrification processes, reducing nitrate to dinitrogen gas.[91] This Proteobacterium demonstrates inhibitory effects against *V. parahemolitycus* and *V. alginolyticus* in aquatic organisms.[88] In the intestine of *Artemia*, *P. stutzeri* has been described as a probiotic that protects against *Vibrio* sp.[89] In *P. monodon,* it enhances growth, survival, and immunity.[90] The decrease in the relative abundance or the loss of certain bacterial species destabilizes the bacterial community,[87, 92] leading to a significant reduction in the gut microbial diversity.[27, 29, 93] One possible explanation for this pattern is that pathogen colonization outcompetes gut commensals, resulting in lower diversity.[94] According to

this criterion, WSSV infection in shrimp leads to a more divergent intestinal bacterial community.[95]

The PCoA analysis revealed a positive correlation between the increase in viral load (VL), the overexpression of the LDH and AP-2 genes, and changes in the microbiome, providing evidence of the relationship between the microbiome-immune response-energy axis in response to early WSSV infection.

Conclusions

This study represents the first approach to evaluating alterations in the immune and energetic status of WSSV-infected *L. vannamei* and the changes in the gut microbiota during the first 48 h. During this period, genes associated with the anaerobic metabolism, cell differentiation, cell pathogen internalization, and immune response were upregulated. Moreover, we observed changes in the relative abundance of *Vibrio*, *Shewanella*, *Pseudomonas*, *Aeromonas,* and *Flavobacterium*. Finally, the role of *P. stutzeri* as a probiotic during early WSSV infections is a topic that deserves further investigation regarding its potential impact on host susceptibility and/or resistance to WSSV infection.

Data availability

All relevant data are within the manuscript and its supporting information files.

Acknowledgments

Special thanks are conveyed to the Consejo Nacional de Humanidades, Ciencias y Tecnologías (Conahcyt) for supporting the doctoral studies of the first author (FMS-C) (CVU = 878856), which contributed to the development of this research.

Funding statement

This work has been funded by Conahcyt. (https://secihti.mx/conahcyt/que-es-el-conahcyt/). Project: “Identificación de genes que codifican para proteínas alergénicas en humanos asociados a la ingestión de camarones infectados con el virus de la mancha blanca (WSSV) (Ref. 221734) to RR-C. The funder had no role in study design, data collection and analysis, decision to publish, or preparation of the manuscript.

Conflicts of interest

The authors have no conflicts of interest to declare regarding this publication.

Author contributions

Conceptualization: FM Segura-Cadiz, R Rodríguez-Canul.

Data curation: FM Segura-Cadiz, JA Zamora-Briseño, D Cerqueda-García.

Formal analysis: FM Segura-Cadiz, JA Zamora-Briseño, A Hernández-Pérez.

Funding acquisition: R Rodríguez-Canul, G. Gaxiola-Cortés.

Investigation: FM Segura-Cadiz, R Rodríguez-Canul, JA Zamora-Briseño.

Methodology: FM Segura-Cadiz, JA Zamora-Briseño, A Hernández-Pérez, JA Pérez-Vega, M Valenzuela-Jiménez, G Gaxiola-Cortés, D Cerqueda-García, JL Montero-Muñoz.

Project administration: R Rodríguez-Canul.

Resources: R Rodríguez-Canul, G. Gaxiola-Cortés.

Software: FM Segura-Cadiz, JA Zamora-Briseño, A Hernández-Pérez.

Supervision: R Rodríguez-Canul, JA Zamora-Briseño

Validation: FM Segura-Cadiz, D Cerqueda-García, JL Montero-Muñoz.

Visualization: FM Segura-Cadiz, R. Rodríguez-Canul.

Writing-original draft: FM Segura-Cadiz.

Writing-review and editing: All the authors.

References

1. Stentiford GD, Oidtmann B, Scott A, Peeler EJ. Crustacean diseases in European legislation: Implications for importing and exporting nations. Aquaculture. 2010;306(1−4):27–34. doi: 10.1016/j.aquaculture.2010.06.004.
2. Asche F, Anderson JL, Botta R, Kumar G, Abrahamsen EB, Nguyen LT, *et al.* The economics of shrimp disease. Journal of Invertebrate Pathology. 2021;186:107397. doi: 10.1016/j.jip.2020.107397.
3. Zhang Y, Song L, Zhao J, Wang L, Kong P, Liu L, *et al.* Protective immunity induced by CpG ODNs against white spot syndrome virus (WSSV) via intermediation of virus replication indirectly in *Litopenaeus vannamei*. Developmental & Comparative Immunology. 2010;34(4):418–424. doi: 10.1016/j.dci.2009.11.012.
4. Jiravanichpaisal P, Söderhäll K, Söderhäll I. Characterization of white spot syndrome virus replication in *in vitro*-cultured haematopoietic stem cells of freshwater crayfish, *Pacifastacus leniusculus*. Journal of General Virology. 2006;87(4):847–854. doi: 10.1099/vir.0.81758-0.
5. Mayor S, Presley JF, Maxfield FR. Sorting of membrane components from endosomes and subsequent recycling to the cell surface occurs by a bulk flow process. The Journal of Cell Biology. 1993;121(6):1257–1269. doi: 10.1083/jcb.121.6.1257.
6. McMahon HT, Boucrot E. Molecular mechanism and physiological functions of clathrin-mediated endocytosis. Nature Reviews Molecular Cell Biology. 2011;12(8):517–533. doi: 10.1038/nrm3151.

7. Aguilar RC, Ohno H, Roche KW, Bonifacino JS. Functional domain mapping of the clathrin-associated adaptor medium chains 1 and 2. Journal of Biological Chemistry. 1997;272(43):27160–27166. doi: 10.1074/jbc.272.43.27160.

8. Rapoport I, Chen YC, Cupers P, Shoelson SE, Kirchhausen T. Dileucine-based sorting signals bind to the beta chain of AP-1 at a site distinct and regulated differently from the tyrosine-based motif-binding site. The EMBO Journal 1998;17(8):2148–2155. doi: 10.1093/emboj/17.8.2148.

9. Mousavi SA, Malerød L, Berg T, Kjeken R. Clathrin-dependent endocytosis. Biochemical Journal. 2004;377(1):1–16. doi: 10.1042/bj20031000.

10. Kobiler O, Drayman N, Butin-Israeli V, Oppenheim A. Virus strategies for passing the nuclear envelope barrier. Nucleus. 2012;3(6):526–539. doi: 10.4161/nucl.21979.

11. Sánchez-Paz A. White spot syndrome virus: an overview on an emergent concern. Veterinary Research. 2010;41(6):43. doi: 10.1051/vetres/2010015.

12. Huang X, Madan A. CAP3: a DNA sequence assembly program. Genome Research. 1999;9(9):868–877. doi: 10.1101/gr.9.9.868.

13. Wongpanya R, Aoki T, Hirono I, Yasuike M, Tassanakajon A. Analysis of gene expression in haemocytes of shrimp *Penaeus monodon* challenged with white spot syndrome virus by cDNA microarray. Science Asia. 2007;33:165–174. doi: 10.2306/scienceasia1513-1874.2007.33.165.

14. Wang X-F, Liu Q-H, Wu Y, Huang J. *Litopenaeus vannamei* clathrin coat AP17 involved in white spot syndrome virus infection. Fish & Shellfish Immunology. 2016;52:309–316. doi: 10.1016/j.fsi.2016.03.007.

15. Hernández-Pérez A, Zamora-Briseño JA, Ruiz-May E, Pereira-Santana A, Elizalde-Contreras JM, Pozos-González S, *et al.* Proteomic profiling of the white shrimp *Litopenaeus vannamei* (Boone, 1931) hemocytes infected with white spot syndrome virus reveals the induction of allergy-related proteins. Developmental & Comparative Immunology. 2019;91:37–49. doi: 10.1016/j.dci.2018.10.002.

16. Diamantino TC, Almeida E, Soares AMVM, Guilhermino L. Lactate dehydrogenase activity as an effect criterion in toxicity tests with *Daphnia magna* straus. Chemosphere. 2001;45(4−5):553−560. doi: 10.1016/s0045-6535(01)00029-7.

17. Soñanez-Organis JG, Rodriguez-Armenta M, Leal-Rubio B, Peregrino-Uriarte AB, Gómez-Jiménez S, Yepiz-Plascencia G. Alternative splicing generates two lactate dehydrogenase subunits differentially expressed during hypoxia via HIF-1 in the shrimp *Litopenaeus vannamei*. Biochimie. 2012;94(5):1250−1260. doi: 10.1016/j.biochi.2012.02.015.

18. Hernández-Palomares MLE, Godoy-Lugo JA, Gómez-Jiménez S, Gámez-Alejo LA, Ortiz RM, Muñoz-Valle JF, *et al.* Regulation of lactate dehydrogenase in response to WSSV infection in the shrimp *Litopenaeus vannamei*. Fish & Shellfish Immunology. 2018;74:401−409. doi: 10.1016/j.fsi.2018.01.011.

19. Lin X, Kim Y-A, Lee BL, Söderhäll K, Söderhäll I. Identification and properties of a receptor for the invertebrate cytokine astakine, involved in hematopoiesis. Experimental Cell Research. 2009;315(7):1171−1180. doi: 10.1016/j.yexcr.2009.01.001.

20. Liang Y, Xu M-L, Wang X-W, Gao X-X, Cheng J-J, Li C, *et al.* ATP synthesis is active on the cell surface of the shrimp *Litopenaeus vannamei* and is suppressed by WSSV infection. Virology Journal. 2015;12(1):49. doi: 10.1186/s12985-015-0275-7.

21. Armstrong PB, Quigley JP. α 2 -macroglobulin: an evolutionarily conserved arm of the innate immune system. Developmental & Comparative Immunology. 1999;23(4−5):375−390. doi: 10.1016/s0145-305x(99)00018-x.

22. Aspán A, Hall M, Söderhäll K. The effect of endogeneous proteinase inhibitors on the prophenoloxidase activating enzyme, a serine proteinase from crayfish haemocytes. Insect Biochemistry. 1990;20(5):485−492. doi: 10.1016/0020-1790(90)90030-x.

23. Buresova V, Hajdusek O, Franta Z, Sojka D, Kopacek P. IrAM—An α2-macroglobulin from the hard tick *Ixodes ricinus*: Characterization and function in phagocytosis of a potential pathogen *Chryseobacterium indologenes*. Developmental & Comparative Immunology. 2009;33(4):489−498. doi: 10.1016/j.dci.2008.09.011.

24. Belkaid Y, Hand TW. Role of the microbiota in immunity and inflammation. Cell. 2014;157(1):121−141. doi: 10.1016/j.cell.2014.03.011.

25. Lin L, Zhang J. Role of intestinal microbiota and metabolites on gut homeostasis and human diseases. BMC Immunology. 2017;18(1):2. doi: 10.1186/s12865-016-0187-3.

26. Clarke G, Stilling RM, Kennedy PJ, Stanton C, Cryan JF, Dinan TG. Minireview: gut microbiota: the neglected endocrine organ. Molecular Endocrinology. 2014;28(8):1221−1238. doi: 10.1210/me.2014-1108.

27. Xiong J, Zhu J, Dai W, Dong C, Qiu Q, Li C. Integrating gut microbiota immaturity and disease-discriminatory taxa to diagnose the initiation and severity of shrimp disease. Environmental Microbiology. 2017;19(4):1490−1501. doi: 10.1111/1462-2920.13701.

28. Cornejo-Granados F, Lopez-Zavala AA, Gallardo-Becerra L, Mendoza-Vargas A, Sánchez F, Vichido R, *et al.* Microbiome of Pacific Whiteleg shrimp reveals differential bacterial community composition between wild, aquacultured and AHPND/EMS outbreak conditions. Scientific Reports. 2017;7(1):11783. doi: 10.1038/s41598-017-11805-w.

29. Chen W-Y, Ng TH, Wu J-H, Chen J-W, Wang H-C. Microbiome dynamics in a shrimp grow-out pond with possible outbreak of acute hepatopancreatic necrosis disease. Scientific Reports. 2017;7(1):9395. doi: 10.1038/s41598-017-09923-6.

30. Yu W, Wu J-H, Zhang J, Yang W, Chen J, Xiong J. A meta-analysis reveals universal gut bacterial signatures for diagnosing the incidence of shrimp disease. FEMS Microbiology Ecology. 2018;94(10):147. doi: 10.1093/femsec/fiy147.

31. Wang J, Huang Y, Xu K, Zhang X, Sun H, Fan L, *et al.* White spot syndrome virus (WSSV) infection impacts intestinal microbiota composition and function in *Litopenaeus vannamei*. Fish & Shellfish Immunology. 2019;84:130−137. doi: 10.1016/j.fsi.2018.09.076.

32. Gracia-Valenzuela MH, Coronado-Molina D, Hernández-López J, Gollas-Galván T. A simple method for purifying the White Spot Syndrome Virus using ultrafiltration. Aquaculture Research. 2009;40(6):737−743. doi: 10.1111/j.1365-2109.2008.02155.x.

33. Vargas-Albores F, Hernández-López J, Gollas-Galván T, Montaño-Pérez K, Jiménez-Vega F, Yepiz-Plascencia G. Activation of shrimp cellular defence functions by

microbial products. In: Flegel TW, editor. Advances in Shrimp Biotechnology. Bangkok (Thailand): National Center for Genetic Engineering and Biotechnology; 1998. pp. 161–166.

34. Wang H-C, Wang H-C, Leu J-H, Kou G-H, Wang AH-J, Lo C-F. Protein expression profiling of the shrimp cellular response to white spot syndrome virus infection. Developmental & Comparative Immunology. 2007;31(7):672−686. doi: 10.1016/j.dci.2006.11.001.

35. Zhang L, Orth K. Virulence determinants for *Vibrio parahaemolyticus* infection. Current Opinion in Microbiology. 2013;16(1):70−77. doi: 10.1016/j.mib.2013.02.002.

36. Liang G-F, Liang Y, Xue Q, Lu J-F, Cheng J-J, Huang J. Astakine LvAST binds to the β subunit of F_1-ATP synthase and likely plays a role in white shrimp *Litopeneaus vannamei* defense against white spot syndrome virus. Fish & Shellfish Immunology. 2015;43(1):75−81. doi: 10.1016/j.fsi.2014.12.015.

37. Motley AM, Berg N, Taylor MJ, Sahlender DA, Hirst J, Owen DJ, *et al.* Functional analysis of AP-2 α and μ2 subunits. Molecular Biology of the Cell. 2006;17(12):5298−5308. doi: 10.1091/mbc.e06-05-0452.

38. Lin Y-C, Vaseeharan B, Chen J-C. Molecular cloning and phylogenetic analysis on α2-macroglobulin (α2-M) of white shrimp *Litopenaeus vannamei*. Developmental & Comparative Immunology. 2008;32(4):317−329. doi: 10.1016/j.dci.2007.07.002.

39. Valenzuela-Castillo A, Mendoza-Cano F, Enríquez-Espinosa T, Grijalva-Chon JM, Sánchez-Paz A. Selection and validation of candidate reference genes for quantitative real-time PCR studies in the shrimp *Penaeus vannamei* under viral infection. Molecular and Cellular Probes. 2017;33:42−50. doi: 10.1016/j.mcp.2017.02.005.

40. Klindworth A, Pruesse E, Schweer T, Peplies J, Quast C, Horn M, *et al.* Evaluation of general 16S ribosomal RNA gene PCR primers for classical and next-generation sequencing-based diversity studies. Nucleic Acids Research. 2013;41(1):e1. doi: 10.1093/nar/gks808.

41. Pfaffl MW. A new mathematical model for relative quantification in real-time RT-PCR. Nucleic Acids Research. 2001;29(9):e45. doi: 10.1093/nar/29.9.e45.

42. Livak KJ, Schmittgen TD. Analysis of relative gene expression data using real-time quantitative PCR and the $2^{-\Delta\Delta C_T}$ method. Methods. 2001;25(4):402−408. doi: 10.1006/meth.2001.1262.

43. Pfaffl MW, Horgan GW, Dempfle L. Relative expression software tool (REST©) for a group-wise comparison and statistical analysis of relative expression results in real-time PCR. Nucleic Acids Research. 2002;30(9):e36. doi: 10.1093/nar/30.9.e36.

44. McKight PE, Najab J. Kruskal-Wallis test. In: IB Weiner, WE Craighead, editors. The Corsini Encyclopedia of Psychology. Hoboken, NJ: Wiley Online Library. 2010. p. 1. doi: 10.1002/9780470479216.corpsy0491.

45. Caporaso JG, Kuczynski J, Stombaugh J, Bittinger K, Bushman FD, Costello EK, *et al.* QIIME allows analysis of high-throughput community sequencing data. Nature Methods. 2010;7(5):335−336. doi: 10.1038/nmeth.f.303.

46. Callahan BJ, McMurdie PJ, Rosen MJ, Han AW, Johnson AJA, Holmes SP. DADA2: High-resolution sample inference from Illumina amplicon data. Nature Methods. 2016;13(7):581−583. doi: 10.1038/nmeth.3869.

47. Rognes T, Flouri T, Nichols B, Quince C, Mahé F. VSEARCH: a versatile open source tool for metagenomics. PeerJ. 2016;4:e2584. doi: 10.7717/peerj.2584.

48. Segata N, Izard J, Waldron L, Gevers D, Miropolsky L, Garrett WS, *et al.* Metagenomic biomarker discovery and explanation. Genome Biology. 2011;12(6):R60. doi: 10.1186/gb-2011-12-6-r60.

49. Legendre P, De Cáceres M. Beta diversity as the variance of community data: dissimilarity coefficients and partitioning. Ecology Letters. 2013;16(8):951−963. doi: 10.1111/ele.12141.

50. Oksanen J, Simpson GL, Blanchet FG, Kindt R, Legendre P, Minchin PR, *et al.* Vegan: community ecology package (2.6-2). Vienna, Austria: R Foundation for Statistical Computing. 2022. 295 pp.

51. Li F, Li M, Ke W, Ji Y, Bian X, Yan X. Identification of the immediate-early genes of white spot syndrome virus. Virology. 2009;385(1):267−274. doi: 10.1016/j.virol.2008.12.007.

52. Han F, Xu J, Zhang X. Characterization of an early gene (wsv477) from shrimp white spot syndrome virus (WSSV). Virus Genes. 2007;34(2):193−198. doi: 10.1007/s11262-006-0053-0.

53. Verbruggen B, Bickley LK, Van Aerle R, Bateman KS, Stentiford GD, Santos EM, *et al.* Molecular mechanisms of white spot syndrome virus infection and perspectives on treatments. Viruses. 2016;8(1):23. doi: 10.3390/v8010023.

54. Friesen PD. Regulation of baculovirus early gene expression. In: Miller LE, editor. The Baculoviruses. The Viruses. Boston, MA: Springer Nature. 1997. pp. 141−170. doi: 10.1007/978-1-4899-1834-5_6.

55. Sánchez-Martínez JG, Aguirre-Guzmán G, Mejía-Ruíz H. White spot syndrome virus in cultured shrimp: A review. Aquaculture Research. 2007;38(13):1339−1354. doi: 10.1111/j.1365-2109.2007.01827.x.

56. Yi G, Wang Z, Qi Y, Yao L, Qian J, Hu L. Vp28 of shrimp white spot syndrome virus is involved in the attachment and penetration into shrimp cells. BMB Reports. 2004;37(6):726−734. doi: 10.5483/bmbrep.2004.37.6.726.

57. OIE. Enfermedades de la Lista de la OIE 2019. Oficina Internacional de Epizootias. 2019. https://www.woah.org/fileadmin/Home/esp/Health_standards/aahm/current/2.2.08_WSD_ESP.pdf

58. Mowery YM, Pizzo SV. The antitumorigenic trifecta. Blood. 2009;114(9):1727−1728. doi: 10.1182/blood-2009-06-226233.

59. Chen I-T, Aoki T, Huang Y-T, Hirono I, Chen T-C, Huang J-Y, *et al.* White spot syndrome virus induces metabolic changes resembling the Warburg effect in shrimp hemocytes in the early stage of infection. Journal of Virology. 2011;85(24):12919−12928. doi: 10.1128/jvi.05385-11.

60. Su M-A, Huang Y-T, Chen I-T, Lee D-Y, Hsieh Y-C, Li C-Y, *et al.* An invertebrate Warburg effect: a shrimp virus achieves successful replication by altering the host metabolome via the PI3K-Akt-mTOR pathway. PLOS Pathogens 2014;10(6):e1004196. doi: 10.1371/journal.ppat.1004196.

61. Fregoso-Peñuñuri AA, Valenzuela-Soto EM, Figueroa-Soto CG, Peregrino-Uriarte AB, Ochoa-Valdez M, Leyva-Carrillo L, *et al.* White shrimp *Litopenaeus vannamei*

recombinant lactate dehydrogenase: Biochemical and kinetic characterization. Protein Expression and Purification. 2017;137:20−25. doi: 10.1016/j.pep.2017.06.010.

62. Cerenius L, Söderhäll K. The prophenoloxidase-activating system in invertebrates. Immunological Reviews. 2004;198(1):116−126. doi: 10.1111/j.0105-2896.2004.00116.x.

63. Ma H, Wang B, Zhang J, Li F, Xiang J. Multiple forms of alpha-2 macroglobulin in shrimp *Fenneropenaeus chinesis* and their transcriptional response to WSSV or *Vibrio* pathogen infection. Developmental & Comparative Immunology. 2010;34(6):677−684. doi: 10.1016/j.dci.2010.01.014.

64. Tonganunt M, Phongdara A, Chotigeat W, Fujise K. Identification and characterization of syntenin binding protein in the black tiger shrimp *Penaeus monodon*. Journal of Biotechnology. 2005;120(2):135−145. doi: 10.1016/j.jbiotec.2005.06.006.

65. Somboonwiwat K, Chaikeeratisak V, Wang HC, Lo CF, Tassanakajon A. Proteomic analysis of differentially expressed proteins in *Penaeus monodon* hemocytes after *Vibrio harveyi* infection. Proteome Science. 2010;8(1):39. doi: 10.1186/1477-5956-8-39.

66. Perazzolo LM, Bachère E, Rosa RD, Goncalves P, Andreatta ER, Daffre S, *et al.* Alpha2-macroglobulin from an Atlantic shrimp: biochemical characterization, sub-cellular localization and gene expression upon fungal challenge. Fish & Shellfish Immunology. 2011;31(6):938−943. doi: 10.1016/j.fsi.2011.08.011.

67. Shanthi S, Vaseeharan B. Alpha 2 macroglobulin gene and their expression in response to GFP tagged *Vibrio parahaemolyticus* and WSSV pathogens in Indian white

shrimp *Fenneropenaeus indicus*. Aquaculture. 2014;418-419:48−54. doi: 10.1016/j.aquaculture.2013.10.003.

68. Chotigeat W, Deachamag P, Phongdara A. Identification of a protein binding to the phagocytosis activating protein (PAP) in immunized black tiger shrimp. Aquaculture. 2007;271(1−4):112−120. doi: 10.1016/j.aquaculture.2007.03.019.

69. Pan L, Xie P, Hu F. Responses of prophenoloxidase system and related defence parameters of *Litopenaeus vannamei* to low salinity. Journal of Ocean University of China. 2010;9(3):273−278. doi: 10.1007/s11802-010-1711-3.

70. Huang J, Li F, Wu J, Yang F. White spot syndrome virus enters crayfish hematopoietic tissue cells via clathrin-mediated endocytosis. Virology. 2015;486:35−43. doi: 10.1016/j.virol.2015.08.034.

71. Moss SM, LeaMaster BR, Sweeney JN. Relative abundance and species composition of gram-negative, aerobic bacteria associated with the gut of juvenile white shrimp *Litopenaeus vannamei* reared in oligotrophic well water and eutrophic pond water. Journal of the World Aquaculture Society. 2000;31(2):255−263. doi: 10.1111/j.1749-7345.2000.tb00361.x.

72. Oxley APA, Shipton W, Owens L, McKay D. Bacterial flora from the gut of the wild and cultured banana prawn, *Penaeus merguiensis*. Journal of Applied Microbiology. 2002;93(2):214−223. doi: 10.1046/j.1365-2672.2002.01673.x.

73. Liu W-J, Chang Y-S, Wang C-H, Kou G-H, Lo C-F. Microarray and RT-PCR screening for white spot syndrome virus immediate-early genes in cycloheximide-treated shrimp. Virology. 2005;334(2):327−341. doi: 10.1016/j.virol.2005.01.047.

74. Liu H, Wang L, Liu M, Wang B, Jiang K, Ma S, *et al.* The intestinal microbial diversity in Chinese shrimp (*Fenneropenaeus chinensis*) as determined by PCR–DGGE and clone library analyses. Aquaculture. 2011;317(1-4):32−36. doi: 10.1016/j.aquaculture.2011.04.008.

75. Gomez-Gil B, Tron-Mayén L, Roque A, Turnbull JF, Inglis V, Guerra-Flores AL. Species of *Vibrio* isolated from hepatopancreas, haemolymph and digestive tract of a population of healthy juvenile *Penaeus vannamei*. Aquaculture. 1998;163(1−2):1−9. doi: 10.1016/s0044-8486(98)00162-8.

76. Gao S, Pan L, Huang F, Song M, Tian C, Zhang M. Metagenomic insights into the structure and function of intestinal microbiota of the farmed Pacific white shrimp (*Litopenaeus vannamei*). Aquaculture. 2019;499:109−118. doi: 10.1016/j.aquaculture.2018.09.026.

77. De Bruijn I, Liu Y, Wiegertjes GF, Raaijmakers JM. Exploring fish microbial communities to mitigate emerging diseases in aquaculture. FEMS Microbiology Ecology. 2017;94(1):161. doi: 10.1093/femsec/fix161.

78. Sung H-H, Hsu S-F, Chen C-K, Ting Y-Y, Chao W-L. Relationships between disease outbreak in cultured tiger shrimp (*Penaeus monodon*) and the composition of *Vibrio* communities in pond water and shrimp hepatopancreas during cultivation. Aquaculture. 2001;192(2−4):101−110. doi: 10.1016/s0044-8486(00)00458-0.

79. Chatterjee S, Haldar S. *Vibrio* related diseases in aquaculture and development of rapid and accurate identification methods. Journal of Marine Science: Research & Development. 2012;s1:002. doi: 10.4172/2155-9910.s1-002.

80. Xing M, Hou Z, Yuan J, Liu Y, Qu Y, Liu B. Taxonomic and functional metagenomic profiling of gastrointestinal tract microbiome of the farmed adult turbot (*Scophthalmus maximus*). FEMS Microbiology Ecology. 2013;86(3):432−443. doi: 10.1111/1574-6941.12174.

81. Dierckens KR, Vandenberghe J, Beladjal L, Huys G, Mertens J, Swings J. *Aeromonas hydrophila* causes 'black disease' in fairy shrimps (Anostraca; Crustacea). Journal of Fish Diseases. 1998;21(2):113−119. doi: 10.1046/j.1365-2761.1998.00085.x.

82. Zhou J, Fang W, Yang X, Zhou S, Hu L, Li X, *et al.* A nonluminescent and highly virulent *Vibrio harveyi* strain is associated with "bacterial white tail disease" of *Litopenaeus vannamei* shrimp. PloS One. 2012;7(2):e29961. doi: 10.1371/journal.pone.0029961.

83. Rigottier-Gois L. Dysbiosis in inflammatory bowel diseases: the oxygen hypothesis. The ISME Journal. 2013;7(7):1256−1261. doi: 10.1038/ismej.2013.80.

84. Takahashi E, Ozaki H, Fujii Y, Kobayashi H, Yamanaka H, Arimoto S, *et al.* Properties of hemolysin and protease produced by *Aeromonas trota*. PloS One. 2014;9(3):e91149. doi: 10.1371/journal.pone.0091149.

85. Nayak SK. Probiotics and immunity: A fish perspective. Fish & Shellfish Immunology. 2010;29(1):2−14. doi: 10.1016/j.fsi.2010.02.017.

86. Zadeh SS, Saad CR, Christianus A, Kamarudin MS, Sijam K, Shamsudin MN, *et al.* Assessment of growth condition for a candidate probiotic, *Shewanella algae*, isolated from digestive system of a healthy juvenile *Penaeus monodon*. Aquaculture International. 2010;18(6):1017−1026. doi: 10.1007/s10499-010-9319-6.

87. Coyte KZ, Schluter J, Foster KR. The ecology of the microbiome: networks, competition, and stability. Science. 2015;350(6261):663−666. doi: 10.1126/science.aad2602.

88. Abdelkarim M, Kamel C, Fathi K, Amina B. Use of *Pseudomonas stutzeri* and *Candida utilis* in the improvement of the conditions of *Artemia* culture and protection against pathogens. Brazilian Journal of Microbiology. 2010;41(1):107−115. doi: 10.1590/s1517-83822010000100017.

89. Mahdhi A, Harbi B, Esteban MÁ, Chaieb K, Kamoun F, Bakhrouf A. Using mixture design to construct consortia of potential probiotic *Bacillus* strains to protect gnotobiotic *Artemia* against pathogenic *Vibrio*. Biocontrol Science and Technology. 2010;20(9):983–996. doi: 10.1080/09583157.2010.495185.

90. Ibrahem MD. Evolution of probiotics in aquatic world: potential effects, the current status in Egypt and recent prospectives. Journal of Advanced Research. 2015;6(6):765−791. doi: 10.1016/j.jare.2013.12.004.

91. Zumft WG, Braun C, Cuypers H. Nitric oxide reductase from *Pseudomonas stutzeri*. European Journal of Biochemistry 1994;219(1−2):481−490. doi: 10.1111/j.1432-1033.1994.tb19962.x.

92. Mackenzie BW, Waite DW, Hoggard M, Douglas RG, Taylor MW, Biswas K. Bacterial community collapse: a meta-analysis of the sinonasal microbiota in chronic rhinosinusitis. Environmental Microbiology. 2017;19(1):381−392. doi: 10.1111/1462-2920.13632.

93. Dai W, Yu W, Zhang J, Zhu J, Tao Z, Xiong J. The gut eukaryotic microbiota influences the growth performance among cohabitating shrimp. Applied Microbiology and Biotechnology. 2017;101(16):6447−6457. doi: 10.1007/s00253-017-8388-0.

94. Mallon CA, van Elsas JD, Salles JF. Microbial invasions: the process, patterns, and mechanisms. Trends in Microbiology. 2015;23(11):719−729. doi: 10.1016/j.tim.2015.07.013.

95. Hou D, Huang Z, Zeng S, Liu J, Weng S, He J. Comparative analysis of the bacterial community compositions of the shrimp intestine, surrounding water, and sediment. Journal of Applied Microbiology. 2018;125(3):792−799. doi: 10.1111/jam.13919.